Article

Elucidating the Factors Affecting Hydrogen Production Activity Using a CdS/TiO₂ Type-II Composite Photocatalyst

Haruki Nagakawa and Morio Nagata*

Cite This: ACS Omega 2021, 6, 4395−4400

Read Online

ACCESS | Metrics & More | Article Recommendations

ABSTRACT: CdS/TiO₂ is a composite photocatalyst that has been studied over many years and in which electron transfer from CdS to TiO₂ is believed to lead to high photocatalytic activity. However, most reports on improved activity involve hydrogen production in the presence of a sulfide reducing agent. In this study, we comprehensively examined the effects of electron transfer, hydrogen overvoltage, substrate adsorption, and the cocatalyst from relationships between hydrogen production ability and the total number of trapped electrons in the presence of various reducing agents. As a result, we clarified that the electron transfer between CdS and TiO₂ does not necessarily lead to high activity. We showed that the composite photocatalyst needs to be designed for the intended purpose and that evaluating the hydrogen production ability using sacrificial reagents provides insufficient information for use in an actual environment.
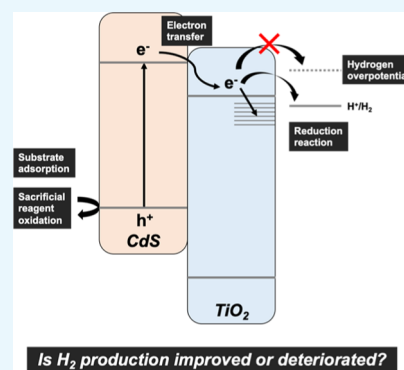
INTRODUCTION

Because sunlight-promoted photocatalytic reactions can proceed through a variety of redox mechanisms, they have attracted attention as solutions to energy depletion and environmental pollution problems.[1,2] In particular, the hydrogen production reaction has attracted attention since water splitting by titanium dioxide (TiO₂) was first reported in 1972.[3] However, a single photocatalyst is often poorly active because of the recombination of excited electrons. The efficiencies of such photocatalytic reactions need to be improved for practical use, and one approach involves combining different photocatalysts;[4,5] in particular, charge transfer can occur between combined photocatalysts with suitable band structures.[6,7] Time-resolved photoluminescence spectroscopy has confirmed that photocatalyst compositing can suppress recombination and prolong electron lifetimes.[8,9] Suppressing recombination improves the hydrogen production rate in the composite compared to that of a single photocatalyst,[8,9] and research into titanium oxide-based composite photocatalysts has been vigorously pursued even in recent years.[10,11] In particular, cadmium sulfide (CdS) and TiO₂ composite photocatalysts, which contain type-II heterojunction structures, are among the most studied combinations. Carrier recombination is suppressed by the movement of excited electrons from the conduction band of CdS to TiO₂ in such a composite,[12,13] which leads to longer electron lifetimes,[14] improved hydrogen production efficiencies,[15,16] and the ability to decompose pigments.[17,18] However, most reports on improving hydrogen production activity using CdS/TiO₂ involve the use of sulfide reducing agents.[15,16,19]

The activity of the photocatalytic reaction is influenced not only by charge transfer but also by other factors, including light absorption, redox reaction and potential, adsorption, desorption, and mass diffusion of the chemical species.[20] Therefore, CdS/TiO₂ composites do not always exhibit superior photocatalytic activities. In this study, we evaluated the abilities of CdS/TiO₂ composites to generate hydrogen in the presence and absence of Na₂S/Na₂SO₃, triethanolamine (TEOA), and methanol (MeOH), as well as the accumulation of excited electrons in electron traps. We comprehensively discuss the factors that influence the photocatalytic reaction on the composite photocatalyst, clarify that CdS/TiO₂ composites do not always exhibit superior activities, and show that the reducing agent is influential. We recommend that composite photocatalysts be custom-designed for the required application, rather than being evaluated using reducing agents as sacrificial reagents.

RESULTS AND DISCUSSION

The X-ray diffractometry (XRD) patterns of pure CdS, TiO₂, and the CdS/TiO₂ composite photocatalyst are shown in Figure 1. Characteristic diffraction peaks of CdS are observed at 2θ values of 26.7, 44.0, and 52.1°, which are indexed to the
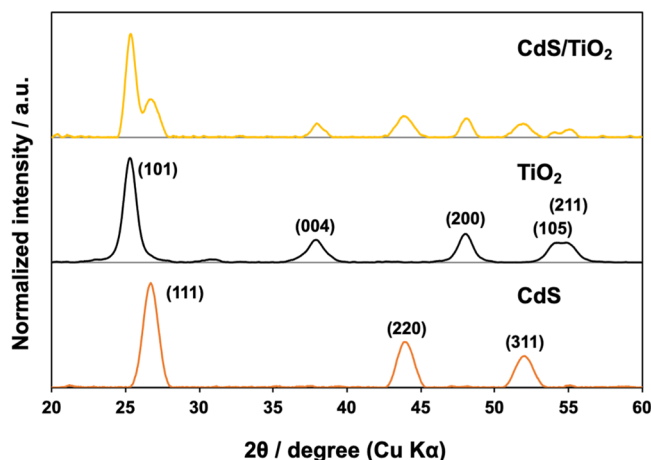
Figure 1. XRD patterns of the prepared CdS, TiO$_2$, and CdS/TiO$_2$ composite.

(111), (220), and (311) crystal planes, respectively, of β-CdS (cubic) (JCPDS PDF no. 04-006-3897). The diffraction peaks detected at 2θ values of 25.3, 37.9, 48.0, 54.2, and 54.8° observed for TiO$_2$ are indexed to the (101), (004), (200), (105), and (211) crystal planes, respectively, of tetragonal anatase TiO$_2$ (JCPDS PDF no. 00-064-0863). On the basis of the peaks observed for the CdS/TiO$_2$ (1:1) composite photocatalyst and its corresponding pure materials, we assume that the prepared composite consists of β-CdS and anatase.

Diffuse reflection spectroscopy (DRS) spectra of the prepared composite and its respective pure materials are shown in Figure 2. The spectrum of CdS/TiO$_2$ is a
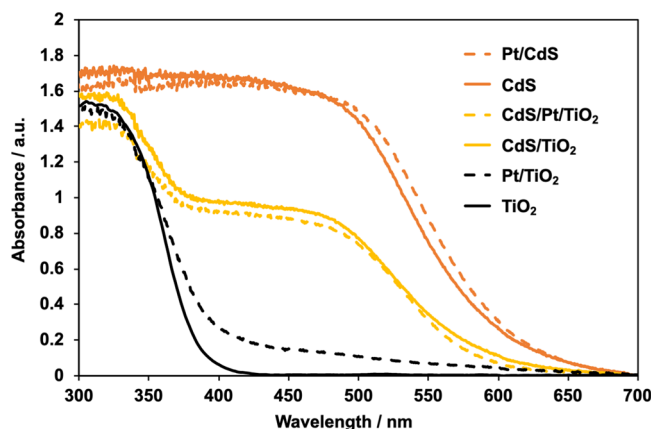

Figure 2. Diffuse reflection spectra of CdS, Pt/CdS, TiO$_2$, Pt/TiO$_2$, CdS/TiO$_2$, and CdS/Pt/TiO$_2$.

combination of those of the individual pure materials. The band gap and absorption edge of each pure material were determined by extrapolating the intersection of the slope and the flattened line of the spectra. The calculated band gaps of CdS and TiO$_2$ were found to be 2.07 and 3.26 eV, respectively, from which the absorption edges were calculated to be 600 and 380 nm, respectively. We confirmed that TiO$_2$ absorbs slightly in the visible region after Pt photodeposition. On the other hand, Pt/CdS and CdS/Pt/TiO$_2$ exhibited almost no changes in absorption.

Figure 3 displays transmission electron microscopy (TEM) images of the prepared photocatalysts. The TEM images of pure TiO$_2$ (Figure 3a) and CdS (Figure 3b) clearly show

agglomerations of fine particles about 5−10 and 10−100 nm in size, respectively. CdS particles with diameters of about 10−100 nm were deposited on the aggregated TiO$_2$ nanoparticles during compositing with CdS (Figure 3c).

Models of the prepared photocatalyst are shown in Figure 4. Pt/CdS and Pt/TiO$_2$ were prepared by photodeposition, while the Pt cocatalyst was deposited only on TiO$_2$ in the case of CdS/Pt/TiO$_2$ because CdS was precipitated on the Pt-deposited TiO$_2$.

Changes in the hydrogen overvoltage in the presence of various reducing agents were investigated by DRS. In these experiments, 1 mm thick quartz cells were filled with TiO$_2$ or CdS/TiO$_2$ powder, after which the powders were separately immersed in solutions containing each reducing agent. The gas in the cell was substituted with Ar and sealed with parafilm. In the case of simple TiO$_2$, the cell was irradiated with a Xe lamp (λ > 380 nm) for 10 min, while CdS/TiO$_2$ was irradiated for 30 min with light of a longer wavelength (λ > 420 nm). Figure 5 shows diffuse reflection spectra of TiO$_2$ in which electrons are trapped upon exposure to light in the presence of each reducing agent. Because the electron traps in TiO$_2$ exist at potentials near the conduction band, the trapped electrons are excited with a lower energy than that required for band gap transition.[21,22] Absorptions from trapped electrons were confirmed by observing wavelengths that are longer than those from the valence band.[23] TiO$_2$ exhibits a bluish color when irradiated with UV light.[23] Compared to the sulfide solution (Figure 5c), the color intensified when MeOH (Figure 5a) or TEOA (Figure 5b) was used as the reducing agent, and the DRS absorption also strengthened (Figure 5d), which is consistent with differences in the total numbers of trapped electrons. Because the same photocatalyst was used, similar electron-trap distributions are expected; hence, the differences in absorption intensity are ascribable to the amounts of unconsumed trapped electrons. Furthermore, because the trapped electrons are consumed through the reduction of protons in the argon atmosphere, the differences in absorption intensity are consistent with differences in the amounts of unconsumed trapped electrons.[21,22] The hydrogen ion concentration on the TiO$_2$ surface decreases with increasing hydrogen overvoltage when the reducing agent adsorbs strongly to TiO$_2$. Therefore, in solutions containing amines (e.g., TEOA) and alcohols (e.g., MeOH), which adsorb somewhat more strongly to TiO$_2$ than water,[24,25] higher hydrogen overvoltages are observed along with higher total numbers of trapped electrons.[26] On the other hand, in the case of a sulfide reducing agent, which adsorbs relatively weakly,[27] a lower hydrogen overvoltage and fewer trapped electrons are observed (Figure 5c).

Figure 6 shows the results of the same experiment performed by irradiating CdS/TiO$_2$ with visible light. The largest increase in absorption wavelength due to trapped electrons was observed for TEOA (Figure 6b), while no change was observed in the case of MeOH (Figure 6a). Because simple CdS absorbs visible light (Figure 2) and electron traps are present on TiO$_2$ (Figure 5), the observed increase in absorption due to trapped electrons is suggestive of electron transfer from CdS to TiO$_2$.[28] Alcohols bind more weakly to CdS than amines and sulfides, which we conclude is the reason why absorption does not increase in the presence of MeOH and oxidation does not occur, with charge recombination proceeding on CdS instead.[29] The complex exhibited the strongest color change in the presence of TEOA (Figure
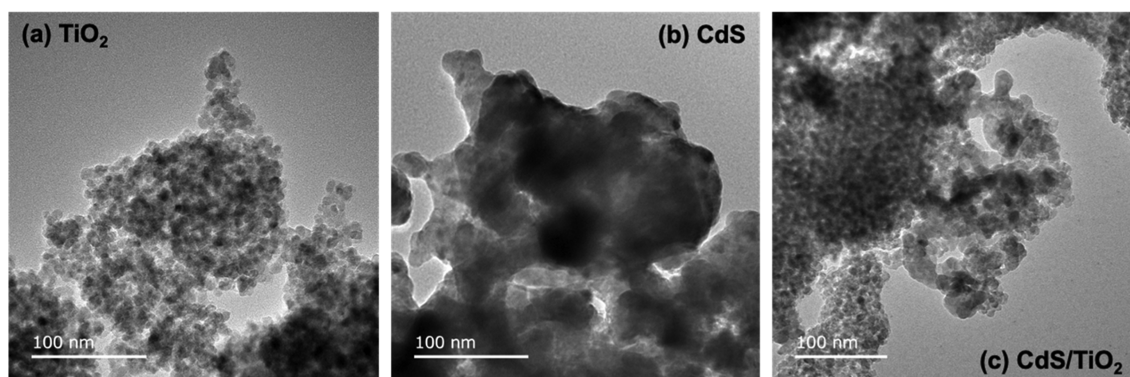
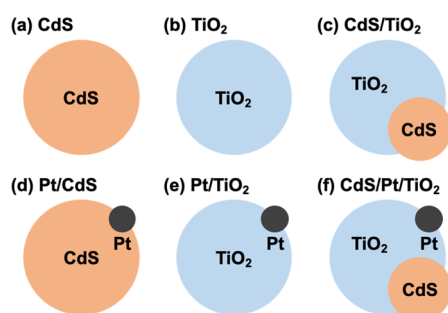**Figure 3.** TEM images of (a) TiO$_2$, (b) CdS, and (c) CdS/TiO$_2$.

Figure 4. Illustration of the prepared photocatalyst. (a) CdS, (b) TiO$_2$, (c) CdS/TiO$_2$, (d) Pt/CdS, (e) Pt/TiO$_2$, and (f) CdS/Pt/TiO$_2$.

suppressed recombination and electron transfer from CdS to TiO$_2$. The Pt cocatalyst was more effective when TiO$_2$ was included, with the hydrogen production rate improved by a factor of 7.1 for Pt−TiO$_2$ alone and 475 times in the case of CdS/Pt/TiO$_2$ because, as shown in Figure 6c, some of the electrons become trapped when the sulfide solution is used as the reducing agent. Because the Pt cocatalyst lowers the hydrogen overvoltage,[30] the excited electrons on TiO$_2$, and the electrons transported from CdS, are effectively used to produce hydrogen.

Entries 7−12 show hydrogen production rates using TEOA as the reducing agent, which show a trend different from that of the sulfide solution. The hydrogen production rate of the CdS/TiO$_2$ composite was reduced to 1/55 of that of simple CdS because, as shown in Figure 6b, TEOA adsorbs more strongly to TiO$_2$ than a sulfide reducing agent; hence, the hydrogen overvoltage is higher and electrons are trapped. Therefore, the hydrogen production rate can effectively be increased by depositing Pt and lowering the hydrogen overvoltage. A similar trend was also observed for simple TiO$_2$.

Entries 13−18 show hydrogen production rates using MeOH as the reducing agent. MeOH is weakly adsorbed to CdS; consequently, no hydrogen was produced on CdS. However, MeOH in the vicinity of CdS was oxidized by its adsorption on the TiO$_2$ surface after compositing with TiO$_2$;

6b), as TEOA is easily adsorbed by both CdS and TiO$_2$; consequently, oxidation proceeds sufficiently with a hydrogen overvoltage.

We next evaluated the photocatalytic activities of the prepared photocatalysts with each reducing agent (Table 1). Entries 1−6 of Table 1 list hydrogen production rates using the sulfide solution as the reducing agent. Compared to simple CdS, the hydrogen production rate was approximately 1.6 times higher when combined with TiO$_2$. We conclude that this improvement in the hydrogen production rate is largely due to
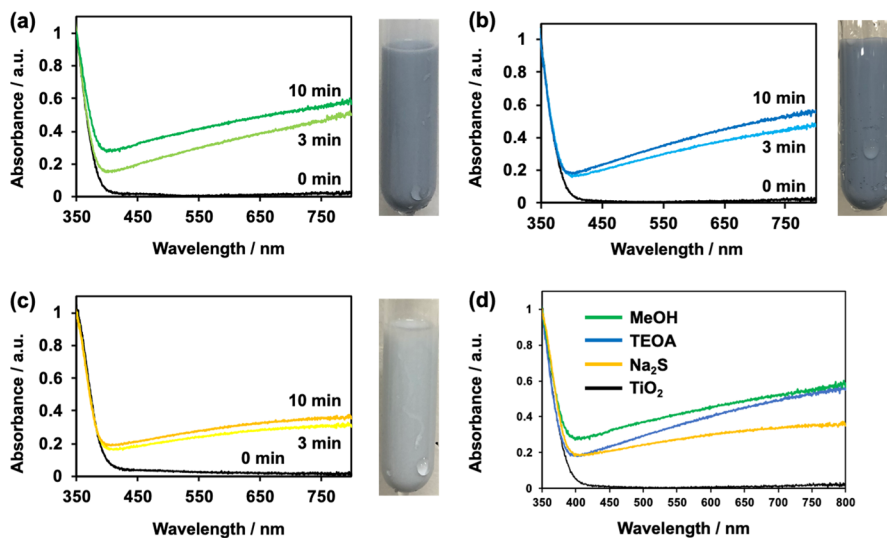

Figure 5. Diffuse reflection spectra of TiO$_2$ when irradiated with light ($\lambda > 380$ nm) for 0, 3, and 10 min in the presence of (a) 50 vol % MeOH, (b) 50 vol % TEOA, (c) 0.1 M Na$_2$S/Na$_2$SO$_3$, and (d) comparison of them.
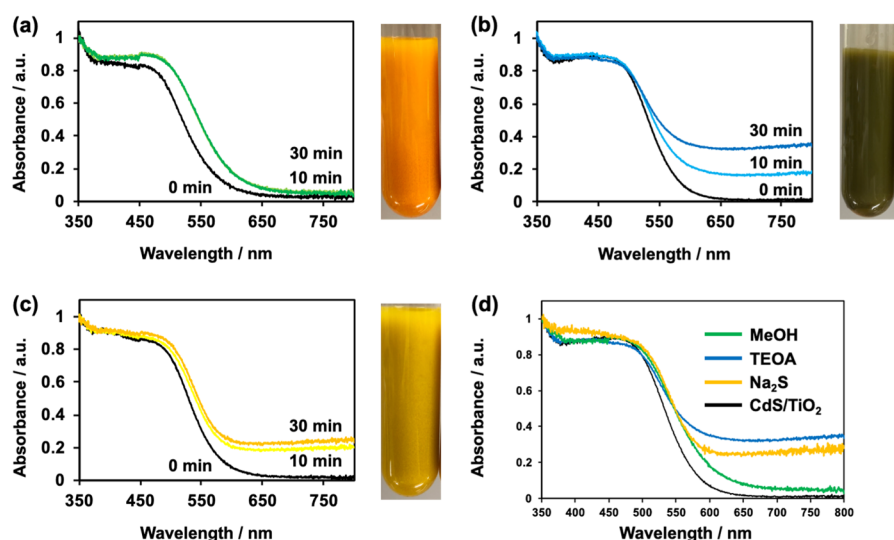
Figure 6. Diffuse reflection spectra of CdS/TiO$_2$ when irradiated with light ($\lambda > 420$ nm) for 0, 10, and 30 min in the presence of (a) 50 vol % MeOH, (b) 50 vol % TEOA, (c) 0.1 M Na$_2$S/Na$_2$SO$_3$, and (d) comparison of them.

Table 1. Photocatalytic Hydrogen Production Activities of the Prepared Photocatalysts in the Presence of Each Reducing Agent

entry	reducing agent	photocatalyst	light source	amount of H$_2$/μmol (g cat)$^{-1}$·h^{-1}
1	Na$_2$S + Na$_2$SO$_3$	CdS	$\lambda > 420$ nm	14.7
2	Na$_2$S + Na$_2$SO$_3$	CdS/TiO$_2$	$\lambda > 420$ nm	23.2
3	Na$_2$S + Na$_2$SO$_3$	TiO$_2$	$\lambda > 380$ nm	2.9
4	Na$_2$S + Na$_2$SO$_3$	Pt-loaded CdS	$\lambda > 420$ nm	31.5
5	Na$_2$S + Na$_2$SO$_3$	Pt-loaded CdS/TiO$_2$	$\lambda > 420$ nm	11028.5
6	Na$_2$S + Na$_2$SO$_3$	Pt-loaded TiO$_2$	$\lambda > 380$ nm	20.6
7	TEOA	CdS	$\lambda > 420$ nm	60.1
8	TEOA	CdS/TiO$_2$	$\lambda > 420$ nm	1.1
9	TEOA	TiO$_2$	$\lambda > 380$ nm	2.5
10	TEOA	Pt-loaded CdS	$\lambda > 420$ nm	332.7
11	TEOA	Pt-loaded CdS/TiO$_2$	$\lambda > 420$ nm	645.8
12	TEOA	Pt-loaded TiO$_2$	$\lambda > 380$ nm	626.0
13	MeOH	CdS	$\lambda > 420$ nm	0.0
14	MeOH	CdS/TiO$_2$	$\lambda > 420$ nm	0.0
15	MeOH	TiO$_2$	$\lambda > 380$ nm	54.3
16	MeOH	Pt-loaded CdS	$\lambda > 420$ nm	0.0
17	MeOH	Pt-loaded CdS/TiO$_2$	$\lambda > 420$ nm	159.7
18	MeOH	Pt-loaded TiO$_2$	$\lambda > 380$ nm	459.5

consequently, hydrogen production was confirmed for the CdS/TiO$_2$ composite with a Pt cocatalyst. As for simple TiO$_2$, its hydrogen production rate was improved by lowering the hydrogen overvoltage with the Pt cocatalyst, in the same manner as TEOA.

The band structure model shown in Figure 7 is proposed based on the results and discussion presented above. Simple CdS has a high conduction band and is not easily affected by the hydrogen overvoltage. Therefore, more strongly adsorbed reducing agents lead to higher hydrogen production activity. On the other hand, simple TiO$_2$ is easily affected by the hydrogen overvoltage because the level of its conduction band is very close to the proton redox potential. Therefore, excessively strong reducing agent adsorption leads to lower activity. When a Pt cocatalyst is deposited on TiO$_2$, the activity is significantly improved to reduce the hydrogen overvoltage. The trapped electrons in the CdS/TiO$_2$ powder composite photocatalyst were evaluated by DRS, which revealed that

electrons are transported from CdS to TiO$_2$. Only CdS is excited when irradiated with visible light; hence oxidation proceeds on CdS. Therefore, stronger reducing agent adsorption on CdS leads to higher activity. Because the TEOA and sulfide reducing agents adsorb more strongly to CdS than MeOH, their hydrogen production activities are higher. On the other hand, the hydrogen overvoltage rises and the reduction reaction becomes disadvantageous if the reducing agent is adsorbed strongly to TiO$_2$, which was remarkably observed for TEOA, as shown in Figure 6b, confirming that hydrogen production activity is reduced by compositing CdS with TiO$_2$.

■ CONCLUSIONS

Designing a photocatalyst that strongly adsorbs the reducing agent on its oxidation side, while weakly adsorbing it on its reduction side is necessary in order to minimize recombination due to electron transfer in a composite photocatalyst. In
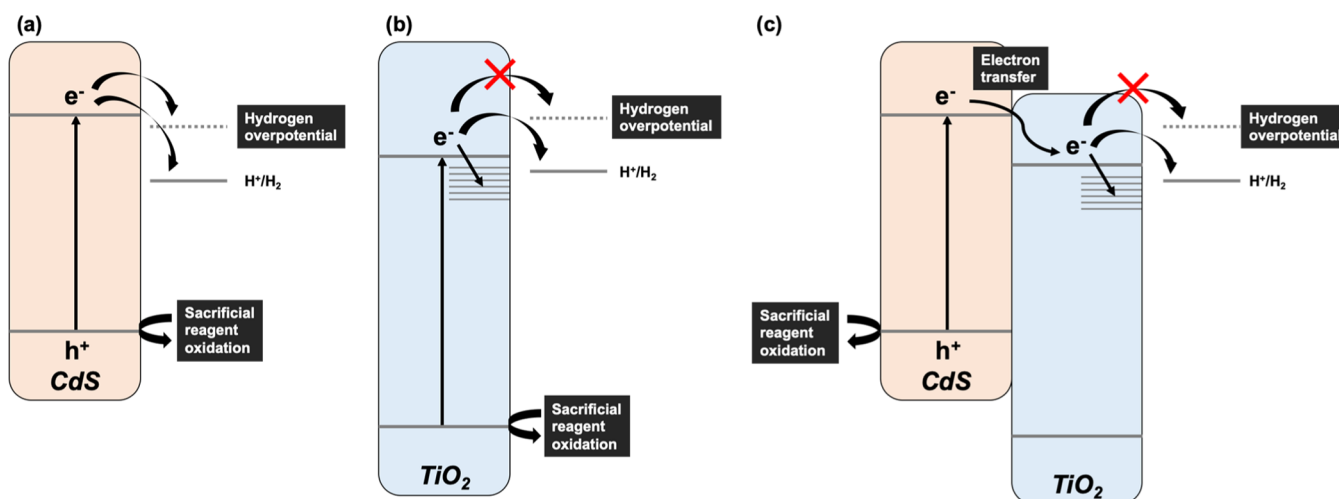
Figure 7. Schematic illustration of the hydrogen production mechanism using (a) CdS, (b) TiO_2, and (c) CdS/TiO_2 in the presence of a reducing agent.

particular, when a photocatalyst (such as TiO_2) selected as the reduction side is strongly affected by the hydrogen overvoltage because the lower end of its conduction band is close to the proton reduction potential, a cocatalyst such as Pt is necessary. In a composite, such as CdS/TiO_2, electron transfer can occur with effectively suppressed recombination, but this depends on the type of reducing agents, as electron transfer may lead to a decrease in activity. In other words, evaluating photocatalytic activity using a reducing agent does not reveal the general characteristics of the catalytic material, but merely its activity as a reducing agent. Therefore, it is necessary to evaluate a catalyst using a reducing agent that is matched to the actual application, and the composite photocatalyst should also be designed and prepared to match that purpose.

EXPERIMENTAL SECTION

Synthesis Method. The CdS/TiO_2 composite photocatalyst was synthesized according to a simple two-step method. First, TiO_2 nanoparticles were synthesized through a sol−gel process at room temperature involving the hydrolysis of titanium isopropoxide (Kanto Chemical Co., Inc., Tokyo, Japan). Titanium isopropoxide was added dropwise to isopropanol, and the solution was stirred for 30 min. Pure H_2O was subsequently added dropwise, and the resulting suspension was stirred for 1 h. The prepared powder was collected by filtration, dried, and calcined at 673 K for 2 h under a flow of air to increase the crystallinity of TiO_2. The CdS/TiO_2 composite photocatalyst was prepared using a facile wet chemistry approach in which 3.08 g of Cd(NO$_3$)$_2$·4H$_2$O (Kanto Chemical Co., Inc., Tokyo, Japan) was dissolved in ethanol (100 mL), after which 0.80 g of the prepared TiO_2 powder was added to the ethanol solution and mechanically stirred for 1 h. A solution of 2.4 g of Na$_2$S·9H$_2$O (Wako Pure Chemical Industries Ltd., Tokyo, Japan) in 20 mL of water was added dropwise to the aforementioned mixture, with agitation continued for 1 h. The formed composite powder was collected by filtration, washed with pure ethanol and ultrapure water, and dried at 393 K for 24 h.

For comparison, pure CdS was prepared using a similar method but with the addition of TiO_2 excluded; in this approach, 0.5 wt % Pt was deposited on simple CdS and TiO_2 using H$_2$PtCl$_6$·6H$_2$O (Kanto Chemical Co., Inc., Tokyo,

Japan) by photodeposition in 0.1 M Na$_2$S and Na$_2$SO$_3$ solution. CdS/Pt/TiO_2 was prepared using a method similar to CdS/TiO_2, with TiO_2 substituted for Pt/TiO_2.

Characterization. The synthesized photocatalysts were characterized by XRD (horizontal sample-type multipurpose X-ray diffractometer, Ultima IV, Rigaku, Tokyo, Japan), DRS (U-3900/3900H spectrophotometer, Hitachi High-Tech Science, Tokyo, Japan), and TEM (EM-002BF, JEM-2100, JEOL, Tokyo, Japan).

Photocatalytic Hydrogen Production Testing. Hydrogen evolution experiments were conducted in test tubes (32 mL) sealed with rubber caps under Ar. The synthesized photocatalyst (50 mg) and an aqueous solution containing the reducing agent (5 mL of 0.1 M Na$_2$S/Na$_2$SO$_3$, 50 vol % TEOA, or 50 vol % MeOH) were prepared in the reaction cell. In order to maintain a constant reaction solution temperature, photocatalytic testing was carried out in a quartz water bath with externally irradiated light. A Xe lamp with a UV cutoff filter ($\lambda > 420$ nm) was used as a visible-light source. A 0.2 mL aliquot of the evolved gas was collected using a gastight syringe and injected into a gas chromatograph (GC-8A, Shimadzu, Japan) to determine the amount of evolved hydrogen. The hydrogen production rate was calculated from the time dependence of the amount of evolved hydrogen over a 2 h period.

AUTHOR INFORMATION

Corresponding Author

Morio Nagata − *Department of Industrial Chemistry, Graduate School of Engineering, Tokyo University of Science, Tokyo 162-0826, Japan;* ⓘ orcid.org/0000-0001-6949-713X; Email: nagata@ci.tus.ac.jp

Author

Haruki Nagakawa − *Department of Industrial Chemistry, Graduate School of Engineering, Tokyo University of Science, Tokyo 162-0826, Japan;* ⓘ orcid.org/0000-0002-5845-8239

Complete contact information is available at:
https://pubs.acs.org/10.1021/acsomega.0c05749

■ **REFERENCES**

(1) Wang, Q.; Domen, K. Particulate Photocatalysts for Light-Driven Water Splitting: Mechanisms, Challenges, and Design Strategies. *Chem. Rev.* **2020**, *120*, 919−985.

(2) Li, C.; Xu, Y.; Tu, W.; Chen, G.; Xu, R. Metal-Free Photocatalysts for Various Applications in Energy Conversion and Environmental Purification. *Green Chem.* **2017**, *19*, 882−899.

(3) Fujishima, A.; Honda, K. Electrochemical Photolysis of Water at a Semiconductor Electrode. *Nature* **1972**, *238*, 37−38.

(4) Moniz, S. J. A.; Shevlin, S. A.; Martin, D. J.; Guo, Z.-X.; Tang, J. Visible-Light Driven Heterojunction Photocatalysts for Water Splitting − a Critical Review. *Energy Environ. Sci.* **2015**, *8*, 731−759.

(5) Marschall, R. Semiconductor Composites: Strategies for Enhancing Charge Carrier Separation to Improve Photocatalytic Activity. *Adv. Funct. Mater.* **2014**, *24*, 2421−2440.

(6) Nagakawa, H.; Ochiai, T.; Nagata, M. Fabrication of CdS/β-SiC/TiO$_2$ Tri-Composites that Exploit Hole- and Electron-Transfer Processes for Photocatalytic Hydrogen Production under Visible Light. *Int. J. Hydrogen Energy* **2018**, *43*, 2207−2211.

(7) Nagakawa, H.; Ochiai, T.; Takekuma, Y.; Konuma, S.; Nagata, M. Effective Photocatalytic Hydrogen Evolution by Cascadal Carrier Transfer in the Reverse Direction. *ACS Omega* **2018**, *3*, 12770−12777.

(8) Zhang, J.; Zhang, M.; Sun, R.-Q.; Wang, X. A Facile Band Alignment of Polymeric Carbon Nitride Semiconductors to Construct Isotype Heterojunctions. *Angew. Chem., Int. Ed.* **2012**, *51*, 10145−10149.

(9) Wang, X.; Xu, Q.; Li, M.; Shen, S.; Wang, X.; Wang, Y.; Feng, Z.; Shi, J.; Han, H.; Li, C. Photocatalytic Overall Water Splitting Promoted by an aα−β phase Junction on Ga$_2$O$_3$. *Angew. Chem., Int. Ed.* **2012**, *51*, 13089−13092.

(10) Li, Y.; Ding, L.; Yin, S.; Liang, Z.; Xue, Y.; Wang, X.; Cui, H.; Tian, J. Photocatalytic H$_2$ Evolution on TiO$_2$ Assembled with Ti$_3$C$_2$ MXene and Metallic 1T-WS$_2$ as Co-catalysts. *Nano-Micro Lett.* **2020**, *12*, 6.

(11) Li, G.; Huang, J.; Chen, J.; Deng, Z.; Huang, Q.; Liu, Z.; Guo, W.; Cao, R. Highly active photocatalyst of Cu$_2$O/TiO$_2$ octahedron for hydrogen generation. *ACS Omega* **2019**, *4*, 3392−3397.

(12) Pan, X.; Xu, Y.-J. Graphene-Templated Bottom-up Fabrication of Ultralarge Binary CdS−TiO$_2$ Nanosheets for Photocatalytic Selective Reduction. *J. Phys. Chem. C* **2015**, *119*, 7184−7194.

(13) Li, J.; Hoffmann, M. W. G.; Shen, H.; Fabrega, C.; Prades, J. D.; Andreu, T.; Hernandez-Ramirez, F.; Mathur, S. Enhanced Photoelectrochemical Activity of an Excitonic Staircase in CdS@TiO$_2$ and CdS@anatase@rutile TiO$_2$ Heterostructures. *J. Mater. Chem.* **2012**, *22*, 20472−20476.

(14) Gopidas, K. R.; Bohorquez, M.; Kamat, P. V. Photophysical and Photochemical Aspects of Coupled Semiconductors Charge-Transfer Processes in Colloidal CdS-TiO$_2$ and CdS-AgI Systems. *J. Phys. Chem.* **1990**, *94*, 6435−6440.

(15) Jang, J. S.; Li, W.; Oh, S. H.; Lee, J. S. Fabrication of CdS/TiO$_2$ Nano-Bulk Composite Photocatalysts for Hydrogen Production from Aqueous H$_2$S Solution under Visible Light. *Chem. Phys. Lett.* **2006**, *425*, 278−282.

(16) Jang, J. S.; Choi, S. H.; Kim, H. G.; Lee, J. S. Location and State of Pt in Platinized CdS/TiO$_2$ Photocatalysts for Hydrogen Production from Water under Visible Light. *J. Phys. Chem. C* **2008**, *112*, 17200−17205.

(17) Li, G.-S.; Zhang, D.-Q.; Yu, J. C. A New Visible-Light Photocatalyst: CdS Quantum Dots Embedded Mesoporous TiO$_2$. *Environ. Sci. Technol.* **2009**, *43*, 7079−7085.

(18) Qian, S.; Wang, C.; Liu, W.; Zhu, Y.; Yao, W.; Lu, X. An Enhanced CdS/TiO$_2$ Photocatalyst with High Stability and Activity: Effect of Mesoporous Substrate and Bifunctional Linking Molecule. *J. Mater. Chem.* **2011**, *21*, 4945−4952.

(19) Yuan, W.; Zhang, Z.; Cui, X.; Liu, H.; Chen, T.; Yuanrui, S. Fabrication of Hollow Mesoporous CdS@TiO$_2$@Au Microspheres with High Photocatalytic Activity for Hydrogen Evolution from Water under Visible Light. *ACS Sustainable Chem. Eng.* **2018**, *6*, 13766−13777.

(20) Hisatomi, T.; Takanabe, K.; Domen, K. Photocatalytic Water-Splitting Reaction from Catalytic and Kinetic Perspectives. *Catal. Lett.* **2015**, *145*, 95−108.

(21) Nitta, A.; Takase, M.; Takashima, M.; Murakami, N.; Ohtani, B. A Fingerprint of Metal-Oxide Powders: Energy-Resolved Distribution of Electron Traps. *Chem. Commun.* **2016**, *52*, 12096−12099.

(22) Nitta, A.; Takashima, M.; Takase, M.; Ohtani, B. Identification and Characterization of Titania Photocatalyst Powders using Their Energy-Resolved Distribution of Electron Traps as a Fingerprint. *Catal. Today* **2019**, *321−322*, 2−8.

(23) Yan, Y.; Shi, W. D.; Peng, W.; Lin, Y. H.; Zhang, C. X.; Li, L. L.; Sun, Y.; Ju, H. X.; Zhu, J. F.; Ma, W. H.; Zhao, J. C. Proton-Free Electron-Trapping Feature of Titanium Dioxide Nanoparticles Without the Characteristic Blue Color. *Commun. Chem.* **2019**, *2*, 88.

(24) Wang, C.-y.; Groenzin, H.; Shultz, M. J. Comparative Study of Acetic Acid, Methanol, and Water Adsorbed on Anatase TiO$_2$ Probed by Sum Frequency Generation Spectroscopy. *J. Am. Chem. Soc.* **2005**, *127*, 9736−9744.

(25) Polunina, I. A.; Isirikyan, A. A.; Polounine, K. E.; Mikhailova, S. S. Water Influence on the Surfactant Adsorption on TiO2. *Colloids Surf., A* **1999**, *160*, 141−146.

(26) Hillson, P. J. Adsorption and the Hydrogen Overpotential. *Trans. Faraday Soc.* **1952**, *48*, 462−473.

(27) Sung, H. K.; Lee, Y.; Kim, W. H.; Lee, S.-J.; Sung, S.-J.; Kim, D.-H.; Han, Y. S. Enhanced Power Conversion Efficiency of Dye-Sensitized Solar Cells by Band Edge Shift of TiO$_2$ Photoanode. *Molecules* **2020**, *25*, 1502.

(28) Zhu, H.; Yang, Q.; Liu, D.; Duanduan, L.; Weining, Z.; Zijing, C.; Xiaoming, W.; Shicheng, Y.; Zhaosheng, L.; Zhigang, Z. Polaron States as a Massive Electron-Transfer Pathway at Heterojunction Interface. *J. Phys. Chem. Lett.* **2020**, *11*, 9184−9194.

(29) Kumaravel, V.; Imam, M.; Badreldin, A.; Chava, R.; Do, J.; Kang, M.; Abdel-Wahab, A. Photocatalytic Hydrogen Production: Role of Sacrificial Reagents on the Activity of Oxide, Carbon, and Sulfide Catalysts. *Catalysts* **2019**, *9*, 276.

(30) Leung, D. Y. C.; Fu, X.; Wang, C.; Ni, M.; Leung, M. K. H.; Wang, X.; Fu, X. Hydrogen Production over Titania-Based Photocatalysts. *ChemSusChem* **2010**, *3*, 681−694.